

1

# 1                   **Distributed acoustic sensing recordings of low-**

## 2                   **frequency whale calls and ship noises offshore**

### 3                   **central Oregon**

4                   William S. D. Wilcock,<sup>1,1a</sup> Shima Abadi,<sup>1,1b</sup> and Brad Lipovsky<sup>2</sup>

5                   <sup>1</sup>*School of Oceanography, University of Washington, Seattle, WA, 98195*

6                   [wilcock@uw.edu](mailto:wilcock@uw.edu) [abadi@uw.edu](mailto:abadi@uw.edu)

7                   <sup>2</sup>*Department of Earth and Space Sciences, University of Washington, Seattle,*

8                   *WA, 98195* [tpl7@uw.edu](mailto:tpl7@uw.edu)

9

10                  Distributed acoustic sensing (DAS) is an optical technique that can measure strain  
11                  changes along an optical fiber to distances of ~100 km with a spatial sensitivity of  
12                  tens of meters. In November 2021, 4-days of DAS data was collected offshore on  
13                  two cables of the Ocean Observatories Initiative Regional Cabled Array that  
14                  extend offshore central Oregon. Numerous 20 Hz fin whale calls, northeast  
15                  Pacific blue whale A and B calls, and ship noises were recorded. This data is  
16                  publicly available to support studies to understand the frequency and spatial  
17                  sensitivity of submarine DAS for low-frequency acoustic monitoring.

18

19                  Keywords: Distributed Acoustic Sensing, Whale Vocalizations, Ship Noise, Fin  
20                  Whale, Blue Whale, Submarine Cable

---

2                  <sup>1a</sup> Author to whom correspondence should be addressed.

3                  <sup>1b</sup> Also at: School of STEM, Division of Engineering and Mathematics, University of Washington,  
4                  Bothell

5

6

21 1. **Introduction**

22 Low frequency sound within the oceans is generated by a wide number  
23 of physical, biological, and anthropogenic sources (Wilcock et al., 2014).

24 These include the wind interacting with the sea-surface, the deformation of sea  
25 ice and icebergs, earthquakes, volcanic activity, baleen whale and fish  
26 vocalizations, ship propellers and machinery, seismic airguns and pile driving.

27 Passive acoustic monitoring of the ocean soundscape is thus a useful tool to  
28 study a variety of processes and to understand the impacts of anthropogenic  
29 activities and changing climate on the ocean environment (Duarte et al., 2021).

30 Since sustained hydro-acoustic observations are challenging and expensive to  
31 obtain offshore, there is strong motivation to explore new technologies that  
32 might enhance our ability to record and characterize sounds within the oceans.

33 Distributed acoustic sensing (DAS) is a relatively new observational  
34 technique that interrogates an optical fiber with repeated laser pulses and  
35 applies interferometry to the Rayleigh backscattered light to measure changes  
36 in strain along the fiber (Hartog, 2017). The method can work to distances of  
37 up to ~100 km and has a spatial resolution of meters and a broad frequency  
38 sensitivity. A DAS fiber optic cable behaves similarly to a long line of closely  
39 spaced single-axis broadband seismometers oriented in the direction of the  
40 fiber, although DAS measures the spatial derivative of ground velocity (i.e.,  
41 rate of change of strain) rather than ground velocity (Hartog, 2017).

42

43        The spatial resolution of DAS measurements is termed the gauge length  
44    and is controlled by both the duration of the laser pulse and length of time over  
45    which each interferometric measurement is averaged. DAS data is commonly  
46    collected with a channel spacing that is much smaller than the gauge length.  
47    Increasing the gauge length decreases spatial resolution and the sensitivity to  
48    short wavelength strain signals but improves the signal to noise of the  
49    measurement and thus allows measurements to greater distance from which the  
50    backscattered light is more attenuated. The temporal resolution is limited by  
51    the two-way travel time of light along the fiber because there should be no  
52    more than one light pulse in the fiber at once. For example, for a 100 km long  
53    fiber, the maximum laser interrogation rate is  $\sim$ 1000 Hz. If the sampling rate is  
54    at least a factor of 2 lower than the maximum laser interrogation rate, then  
55    successive interrogations can be combined to increase signal to noise.

56        Within industry, DAS has been used for a decade to collect vertical  
57    seismic profiles in boreholes (Mateeva et al., 2014). Within academia, DAS is  
58    now widely used for a variety of geophysical applications including earthquake  
59    studies, seismic imaging and glacier deformation, and it also has application in  
60    urban areas for anthropogenic noise sources (Zhan et al., 2019; Lindsey and  
61    Martin, 2021). On land, DAS observations can often take advantage of the  
62    extensive network of dark fibers that have been laid in urban areas and along  
63    transportation corridors to provide growth capacity for telecommunications. In  
64    the oceans, DAS experiments are more challenging because submarine  
65    telecommunications cables do not generally include dark fibers. Spare fibers  
66    in the nearshore portions of cables would be relatively cheap to add but they

67 are of no use for telecommunications without the expensive optical repeaters  
68 that are necessary to transmit signals more than ~300 km.

69        In 2019, three studies documented the utility of submarine DAS for  
70 recording earthquakes and oceanographic signals using data from short tests of  
71 on the research infrastructure of the MARS cabled observatory in Monterey  
72 Bay (Lindsey et al., 2019), the MEUST deep sea cabled observatory in the  
73 Mediterranean off France (Sladen et al., 2019) and a cable in the North Sea off  
74 Belgium (Williams et al., 2019). This pioneering work has spurred a rapid  
75 growth in interest in submarine DAS including its applications to acoustics.

76        Rivet et al. (2021) showed that DAS could be used to track a tanker  
77 passing over the MEUST cable at water depths of both 85 m and 2000 m.  
78 Matsumoto et al. (2021) compared DAS and hydrophone recordings of airgun  
79 signatures using cable extending offshore Japan to >3000 m water depth. They  
80 found both systems were sensitive to airgun signals from 0.1 to tens of Hz  
81 although the DAS had lower signal to noise above a few Hz. A comparison of  
82 airgun recording between DAS on cable at 100-400 m depth and a towed  
83 hydrophone streamer in a shallow Fjord in Norway (Taweesintananon et al.,  
84 2021) showed similar noise levels on both systems. Working with the same  
85 data set, Bouffaut et al. (2022) present DAS recordings of baleen whales at  
86 frequencies up to nearly 100 Hz and demonstrated tracking for animals  
87 swimming near the cable.

88        In this paper, we present an overview of a 4-day public-domain  
89 submarine DAS experiment that was conducted on two cables extending  
90 offshore central Oregon (section 2), demonstrate the capabilities of DAS to

91 recording hydro-acoustic signals (section 3) from fin whale calls (section 3.1),  
92 blue whale calls (section 3.2) and ship noises (section 3.3) and discuss the  
93 preliminary results and opportunities for future research with these acoustic  
94 signals (section 4).

## 95 2. OOI DAS Experiment

96 The Ocean Observatories Initiative Regional Cabled Array (Figure 1,  
97 inset) operates two submarine cables that land at Pacific City, Oregon (Smith et  
98 al., 2018). The northern cable runs ~500 km west to Axial Seamount while the  
99 southern cable extends ~150 km offshore onto the Juan de Fuca plate before  
100 wrapping around to the south and east onto the continental slope and shelf off  
101 Newport, Oregon. Both cables include a single twisted pair of optical fibers  
102 that support 10 Gbps ethernet to primary nodes on the trunk cables that connect  
103 via secondary cables and junction boxes to suites of sensors on the seafloor and  
104 on moorings.

105 From November 1-5, 2021, a scheduled shutdown of the RCA for  
106 maintenance provided an opportunity for a 4-day community fiber sensing  
107 experiment to interrogate the fibers in each cable extending out to the first  
108 optical repeaters, which are located at 1600 m depth 95 km along the south  
109 cable and at 600 m depth 65 km along the north cable (Figure 1). These  
110 nearshore sections of the cables are buried to a nominal depth of 1.5 m depth  
111 below the seafloor. On the south cable DAS data was collected on both fibers  
112 using an Optasense QuantX interrogator and a Silixa IDASv3 system. On the  
113 north cable DAS data was collected on one fiber with a second Optasense

114 QuantX interrogator while a Silixa ULTIMA SM distributed temperature  
 115 sensor was deployed on the other fiber. The data has a total volume of 26 TB  
 116 and can be accessed through a data repository hosted by the University of  
 117 Washington along with information about the experiment configuration and  
 118 data format (<https://oceanobservatories.org/pi-instrument/rapid-a-community-test-of-distributed-acoustic-sensing-on-the-ocean-observatories-initiative-regional-cabled-array/>).  
 120

121 Table 1 summarizes the DAS recording parameters. Although there  
 122 were some intervals of recording at sample rates up to 1000 Hz and with gauge  
 123 lengths down to 3 m, most of the data were collected with a sample rate of 200  
 124 Hz and gauge length of 30-50 m. These parameters were selected to ensure  
 125 sufficient signal to noise to record to near the distal ends of the fibers.

126

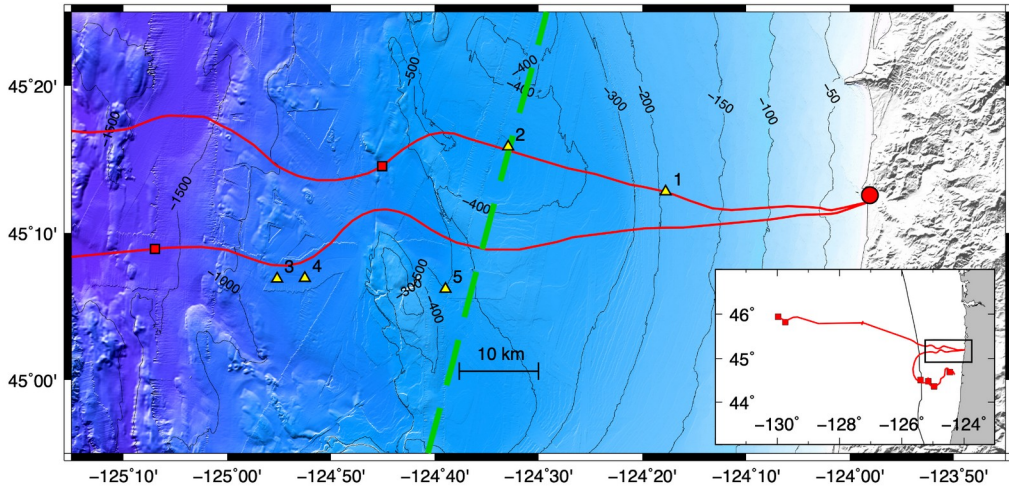
127 TABLE 1. Summary of recording parameters for the OOI RCA DAS  
 128 experiment. For each of the 3 DAS interrogators the table identifies the fiber  
 129 used, the length of fiber interrogated, the channel spacing, the gauge length and  
 130 the sampling frequency with the parameters only listed when they change.

	Optasense - north cable	Optasense - south cable	Silixa - south cable
Nov 1 (2-6 hours)	Testing various configurations	Testing various configurations	Testing on receive fiber of north cable
Nov 1-2	Transmit fiber 65.2 km 2 m channel spacing 30 m gauge length	Transmit Fiber 95 km 2 m channel spacing 50 m gauge length	Receive Fiber 80.6 km 2 m channel spacing 30 m gauge

	1000 Hz sampling	200 Hz sampling	length 200 Hz sampling
Nov 2-3	500 Hz sampling		40.4 km 1 m channel spacing 10 m gauge length
Nov 3-4	50 m gauge length 200 Hz sampling		19.7 km 3 m gauge length 1000 Hz
Nov 4-5			
Nov 5 (3 hours)	Receive fiber	Receive fiber	Transmit fiber 80.5 km 2 m channel spacing 30 m gauge length 200 Hz

131

132



133

134 Fig. 1. Bathymetric map showing the nearshore portion of the two OOI RCA  
 135 cables as red lines, the shore station as a red circle and the first optical  
 136 repeaters as red squares. Also shown are the fin whale call locations obtained

137 by time difference of arrival for the data shown in Fig. 2c, f (numbered yellow  
138 triangles) and the northward track of the cargo ship for which data is shown in  
139 Fig 4 (bold green dashed line). Contours are labeled in meters and are unevenly  
140 spaced (50 m to 200 m depth, 100 m to 500 m depth and 500 m at larger  
141 depths). The inset map shows the geometry of the complete RCA cable with  
142 primary nodes on the cable as red squares, the area of the main figure as a  
143 black box and the base of the continental slope as a faint black line.

144

### 145 3. Results

146 The unfiltered DAS data (Fig. 2a) is dominated by the long period  
147 signals from ocean surface waves (primary microseisms) in shallow water and  
148 secondary microseisms in deeper water (Sladen et al., 2019; Williams et al.,  
149 2019) but acoustic signals are readily apparent when the records are filtered  
150 above  $\sim$ 10 Hz (Fig. 2b). Acoustic signals can be further enhanced by applying  
151 an  $f$ - $k$  filter to remove signals propagating along the cable at less than the speed  
152 of sound (Fig. 2c)

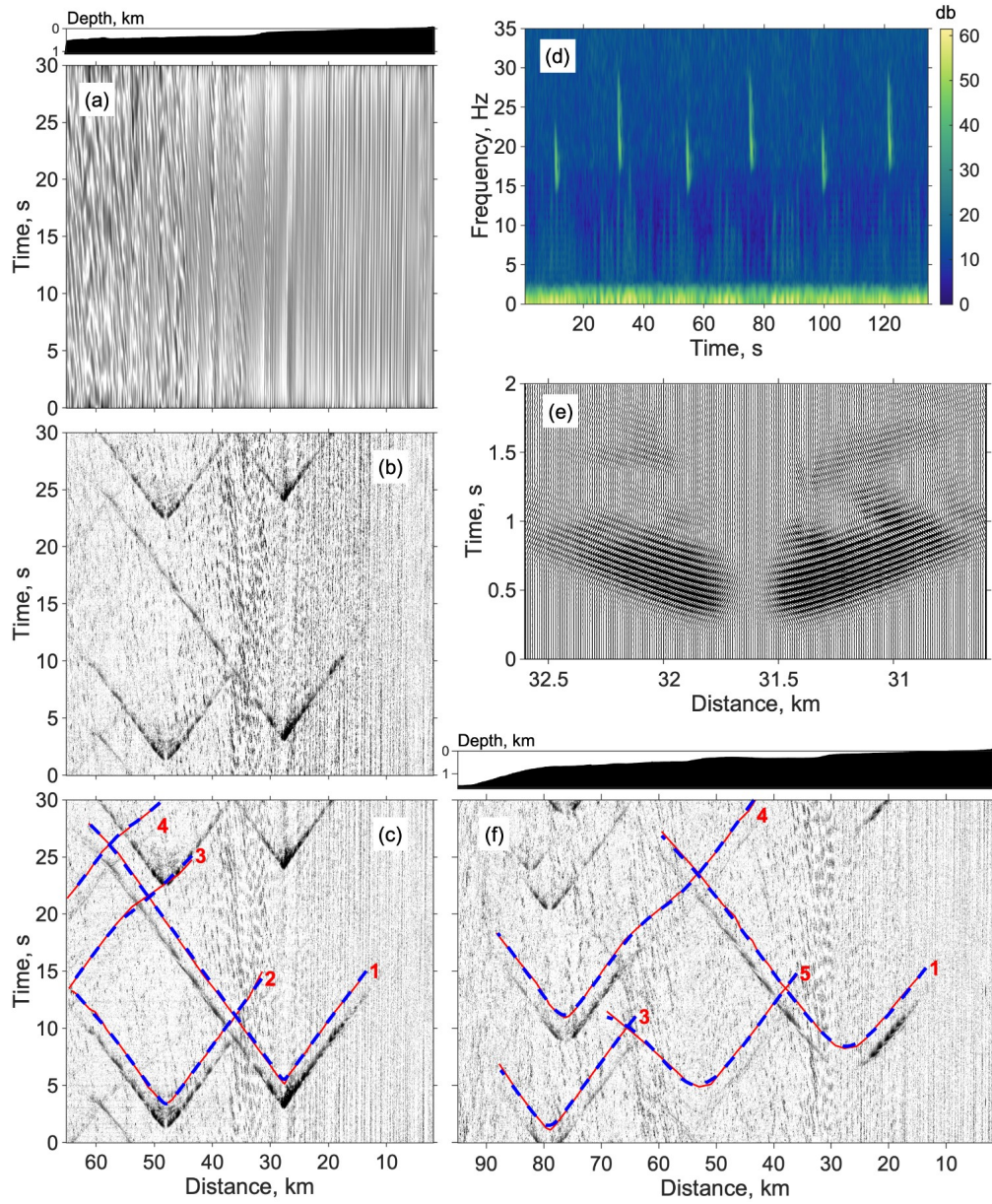
#### 153 2.1. *Fin whale vocalizations*

154 The experiment occurred during the breeding season for fin whales and  
155 songs of the stereotypical 1-s-long 20-Hz fin whale chirp are recorded  
156 throughout. Fin whale calls are observed everywhere along the cables except  
157 within about 10 km of the coast. Individual calls are observed out to distances  
158 of tens of kilometers, forming a characteristic V-shape in the record sections  
159 (Fig 2b-c, f). Spectrograms show that DAS records frequency content of calls

160 with most songs characterized by a doublet pattern of alternating lower and  
161 higher frequency notes (Fig. 2d) that now dominates songs in the northeast  
162 Pacific (Wierathumeller et al., 2017). The recorded amplitudes are low at the  
163 location on the cable closest to the whale (Fig. 2e), as would be expected for a  
164 measurement that is sensitive to strain along rather than across the cable.

165 The fin whale calls can be located using time difference of arrival.

166 Figures 2c, f show an example where vocalizations from 5 whales can be  
167 located at distances that range from 25 km to 75 km offshore and within no  
168 more than a few kilometers of one cable (Fig. 1).



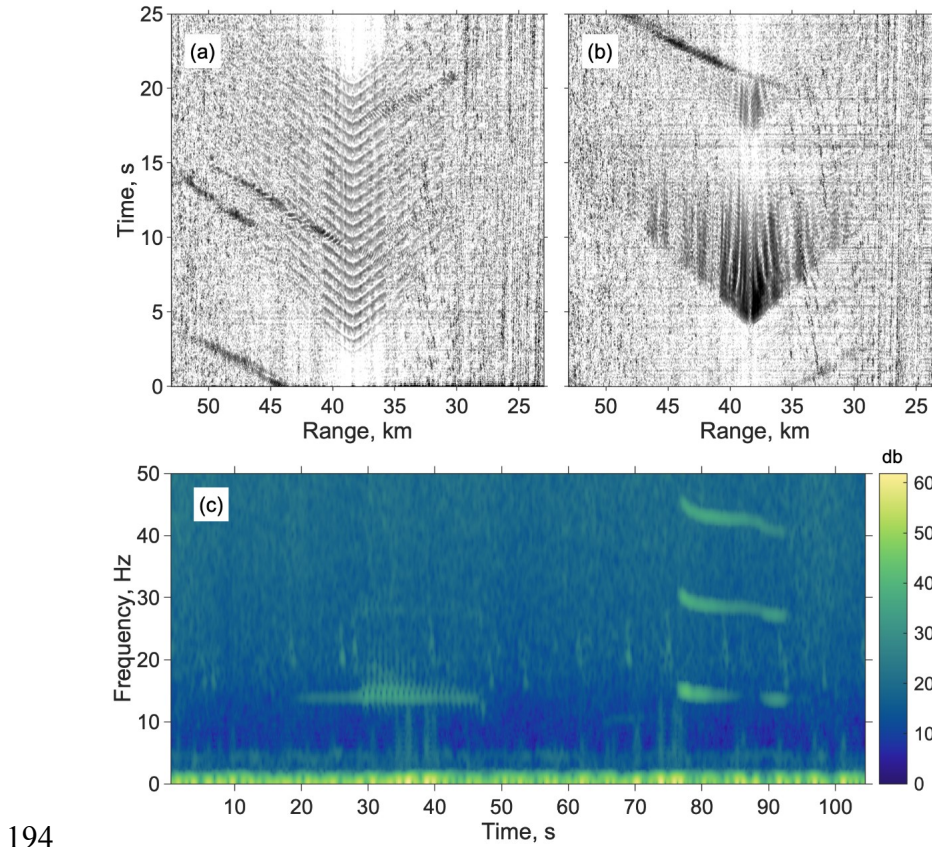
169

170 Fig. 2. Example of fin whale recordings (a) Record section beginning at 04-  
 171 Nov-2021 02:00:27 UT, showing 30 s of unfiltered data recorded by the  
 172 Optasense interrogator on the north cable. Distance from the interrogator is  
 173 plotted on the horizontal axis and time is plotted on the vertical axis with the  
 174 amplitude envelope shown by logarithmically scaled shading after normalizing  
 175 each trace to its median amplitude. (b) As for (a) except after the application

176 of a 15-27 Hz bandpass filter. Fin whale arrivals are visible as dark shaded “V”  
177 shapes with the apex marking the location on the cable closest to the whale.  
178 (c) As for (b) but with a  $f$ - $k$  filter to remove all energy with an apparent  
179 velocity along the cable less than 1.4 km/s. Manual picks of the fin whale  
180 arrivals (red solid line) and model times (bold blue dashed line) for a uniform  
181 velocity of 1.48 km/s are shown offset 2 s from the fin whale calls and are  
182 numbered to indicate the corresponding whale location in Fig. 1. (d)  
183 Spectrogram beginning at 02-Nov-2021 18:15:40 UT, for the Silixa  
184 interrogator on the south cable, averaged over 100 channels, showing 6 notes  
185 in a fin whale doublet song. (e) Record section beginning at 02-Nov-2021  
186 18:16:54 UT, for the Silixa interrogator showing channels within ~1 km of the  
187 closest point to a fin whale call. (f) As for (c) but for the Optasense interrogator  
188 on the south cable.

#### 189.2. *Blue whale vocalizations*

190 The calls of the Northeast Pacific blue whale were much less common  
191 during the experiment, but several sequences of the A and B calls are observed  
192 (Fig. 3) with the first 3 harmonics of the B call well recorded. In contrast to fin  
193 whales, blue whale calls are only recorded out to distances of ~10 km.



194

195 Fig. 3. Example of Northeast Pacific blue whale recordings on the Silixa  
 196 interrogator on the south cable. (a) Record section beginning at 02-Nov-2021  
 197 10:36:09 UT, showing an example of an A call with the closest location on the  
 198 cable at a distance of 38 km. The A call is overlain by several higher  
 199 amplitude fin whale calls. The data have been filtered with a 10.5-18 Hz  
 200 bandpass filter and an  $f$ - $k$  filter to remove energy propagating along the cable at  
 201 less than 1.4 km/s. (b) As for a but showing a B call with record section  
 202 beginning at 02-Nov-2021 10:33:36 UT. Frequency filtering has removed all  
 203 but the first harmonic. (c) Spectrogram beginning at 02-Nov-2021 10:32:24  
 204 UT, averaged over 100 channels, showing an A call followed by a B call.

205

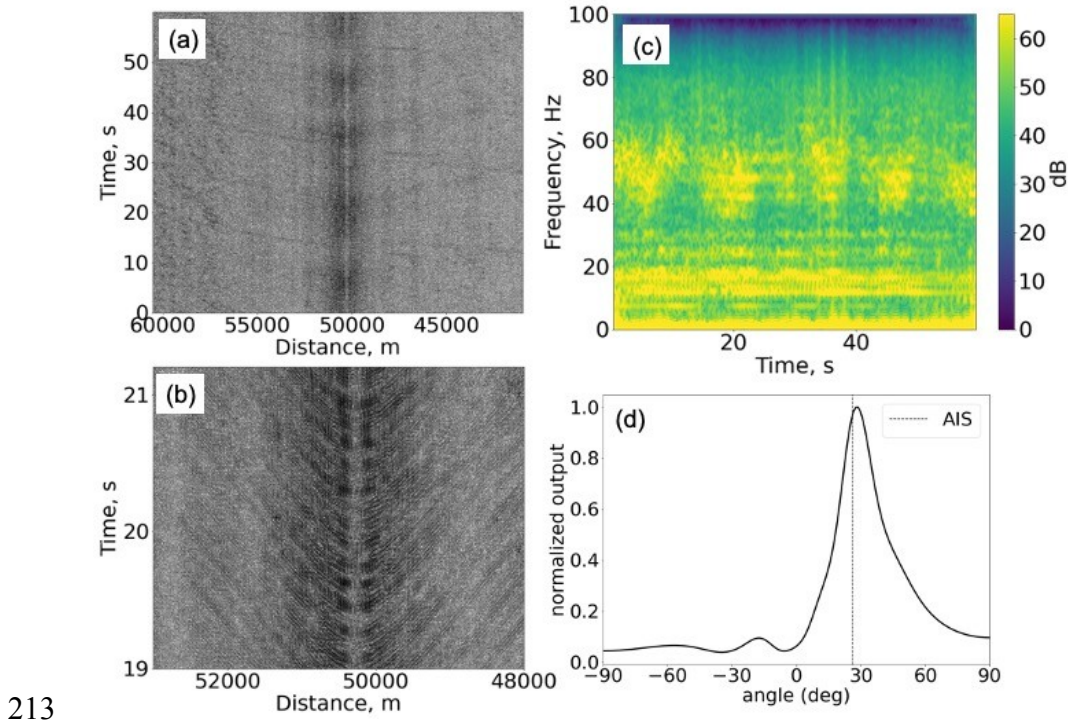
38

39

12

## 206.3. Ship Recordings

207       Figure 4 shows an example of ship noise recorded by the Optasense  
 208    interrogator on both north and south cables. Using the Automatic Identification  
 209    System (AIS) data, this ship was determined to be a cargo ship of length 180 m  
 210    that passes above the cable with an approximate speed of 13.2 knots. The data  
 211    have been filtered with a 10-90 Hz bandpass filter and an  $f$ - $k$  filter to remove  
 212    energy propagating along the cable at less than 1.4 km/s.



213       Fig. 4. Example of ship sound recording beginning at 03-Nov-2021 01:57:31  
 214    UT, traveling at 13.2 knots over both cables recorded by the Optasense  
 215    interrogator with a sample rate of 200 Hz and gauge length of 50 m (a) Record  
 216    section showing 60 s of a cargo ship sound with the closest location on the  
 217    south cable at a distance of 50 km. (b) Record section showing channels within  
 218    21 s.

219 ~5 km of the closest point to the ship. (c) Spectrogram averaged over 100  
220 channels, showing acoustic energy between 10-60 Hz. (d) Plane-wave  
221 beamformer output for the signal shown in (a) using a sub-array of the fiber  
222 optic cable consisting of 150 channels starting at 49.7 km. The estimated  
223 bearing is in agreement with the bearing calculated from the AIS data.

224

225 Compared to fin whale and blue whale calls, ship noises are recorded  
226 over a shorter distance (~5 km). The multipath interferences are noticeable in  
227 Fig. 4b which could be affected by the ship's motion over the cable, varying  
228 coupling of the fiber, different bathymetry along the cable, and fiber curvature.  
229 Similar to Fig. 2e, the recorded amplitudes are low at the location on the cable  
230 closest to the ship (at a distance of 50 km) which is due to the cable sensitivity  
231 to strain along rather than across the cable.

232 Plane-wave beamforming (Jensen et al., 1994) is used to calculate the  
233 bearing of the vessel relative to a 150-channel sub-array between 49.7-50 km.  
234 The beamforming output is maximum at 29.6 degree which is consistent with  
235 the bearing of 26 degree calculated using the ship location from the AIS data.

### 236 3. Discussion

237 The OOI community DAS experiment confirms earlier work which  
238 shows that buried submarine telecommunication cables can record low  
239 frequency acoustic signals. Numerous fin whale calls, blue whale calls, and  
240 ship noises were recorded to distances of up to ~40km, 10 km and 5 km,  
241 respectively.

242 An important question is why these detection distances differ. Studies  
243 suggest that the source levels for fin and blue whales are similar. Average  
244 values of 186 (Watkins et al., 1987), 189 (Wierathmueller et al., 2013) and 171  
245 dB re 1  $\mu$ Pa at 1 m (Charif et al. 2002) have been reported for fin whales in the  
246 northeast Pacific, with the last estimate likely 10-15 dB lower due to the  
247 methodology (Wierathmueller et al., 2013). For the B call of the northeast  
248 Pacific blue whale, reported values are 180 dB (Thode et al., 2000) and 186 dB  
249 re 1  $\mu$ Pa at 1 m (McDonald et al., 2001). While the uncertainties in these  
250 estimates are consistent with fin whale calls being somewhat louder, such an  
251 explanation for the difference in the maximum detection distance in the DAS  
252 data, would be inconsistent with work using ocean bottom seismometers and  
253 hydrophones where blue whale B calls are detected to larger ranges (e.g.,  
254 Wilcock and Hilmo, 2022).

255 The differences may be related to the frequency sensitivity of the DAS  
256 data. First, the optical fiber within an armored buried submarine cable may  
257 couple better to acoustical strain at lower frequencies. Second, DAS  
258 observations average strain changes over the gauge length and when this length  
259 approaches or exceeds the signal wavelength, the summed strain change  
260 measurements will experience aliasing, reducing the recorded amplitude. The  
261 blue whale B call has a significant amount of energy in higher order harmonics  
262 and particularly the 3<sup>rd</sup> harmonic at 40-45 Hz (Thode et al., 2000). The 35 m  
263 wavelength of the 3<sup>rd</sup> harmonic is similar to the 30-50 m gauge length so that at  
264 larger distances, when the call is propagating sub parallel to the cable it may be  
265 poorly recorded.

266 The reported source levels of commercial ships vary from 177-188 dB  
267 re 1  $\mu$ Pa at 1 m (McKenna et al., 2012; MacGillivray and de Jong, 2021) which  
268 suggests that ships have similar or slightly lower source levels than fin and  
269 blue whales. However, ships radiate acoustic energy in a broad frequency  
270 range that can go as high as 1000 Hz with most ships having significant energy  
271 to  $\geq$ 100 Hz. (McKenna et al., 2012). The ship noises recorded in the OOI  
272 DAS experiment do not show acoustic energy above 60 Hz which again would  
273 be consistent with reduced sensitivity at higher frequencies as an explanation  
274 for the lower detection range.

275 Another potential explanation for differences in detection range could  
276 be the depth of the source. Ship propellers are located close to the surface  
277 while studies with acoustical tags show that fin and blue whales vocalize at  
278 depths of up to a few tens of meters (Oleson et al., 2007; Stimpert et al., 2015;  
279 Lewis et al., 2018). With warming ocean surface temperature, the mode  
280 excitation depths move deeper than the typical ship source depths and this can  
281 cause a reduction in the ship noise band spectral level (Dahl et al, 2021).  
282 Additional work is needed to understand the impact of speed of sound profile  
283 on the detection range of different sound source recordings on DAS.

284 The DAS sensitivity, as expected, is strongly directional with the  
285 recorded amplitudes of both whales (Fig. 2c) and ships (Fig. 4d) very low at  
286 the position of closest approach where the propagation direction is  
287 perpendicular to the cable. This effect is understood to be due to the cable-  
288 longitudinal strain rates being insensitive to plane acoustic waves at normal

289 incidence. It also appears from the fin localizations that whales are only clearly  
290 detected on both cables which are spaced ~10 km apart, when the curvature of  
291 the cables results in the call propagating sub-parallel to both cables (e.g.,  
292 locations 3 and 4 in Fig. 1 and the corresponding detections in Fig. 2c, f).

293 The OOI DAS experiment recorded tens of thousands of fin whale  
294 calls, which provide a remarkable data set both to investigate the directional  
295 and depth dependent acoustic sensitivity of DAS near 20 Hz and characterize  
296 the spatial distribution, depth of calling and behavior of vocalizing fin whales  
297 offshore central Oregon. One of the challenges of DAS is determining  
298 accurately the location of each channel, given uncertainties in the path of the  
299 fiber and the speed of light in the fiber. A joint inversion for the location of fin  
300 whale calls and DAS channels would serve as an analog to the tap tests used to  
301 locate fibers on land (Lindsey and Martin, 2021). The fin whale calls can also  
302 be exploited to study low frequency sound propagation with water column  
303 velocity structure potential including this as an unknown in inversions.  
304 Finally, beamforming approaches should be used to explore whether the DAS  
305 data can be used to detect fin whales at azimuths and ranges where they are not  
306 apparent in the filtered plots.

307 The acoustic signals from ships and whales recorded by the OOI DAS  
308 experiment with gauge lengths of 3, 10, 30 and 50 m (Table 1) can be used to  
309 understand frequency sensitivity of DAS at lower frequencies and its  
310 dependence on gauge length. Such work should motivate future experiments  
311 that deploy hydrophones near cables to ground truth recordings and that

312 explore the utility of DAS to detect high-amplitude higher-frequency signals  
313 such as those from humpback or sperm whales.

314 DAS generates large data sets; extrapolating the OOI DAS experiment  
315 to continuous recordings would generate O~2 PB/year of data. To give a sense  
316 of scale, six months of data at this rate is about the size of the entire  
317 Incorporated Research Institutions for Seismology Data Management Center  
318 archive as of April 2022 (<https://ds.iris.edu/data/distribution/>). Managing such  
319 data volumes will require a variety of approaches. Further work is required to  
320 determine optimal channel spacing and to determine whether the 2m channel  
321 spacing used in the OOI experiment is justified by its scientific utility. Other  
322 approaches could involve a return to the triggered data acquisition paradigm  
323 common with seismic data before about the year 2000. A modern approach to  
324 triggered acquisition could leverage smart, potentially machine learning-based  
325 algorithms run in an edge-computing topology so as to only record signals of  
326 interest at high spatial and temporal sampling rates, while still defaulting to a  
327 lower rate data that would enable studies of the ambient field. Both lossy and  
328 lossless real-time data compression should be considered, and recent results  
329 have shown promise in this topic (Dong et al., 2022). The public domain OOI  
330 DAS data provides a resource to support the development of such approaches

331 **Acknowledgments**

332 We thank the technical staff of the OOI RCA and field data acquisition  
333 team for their work to collect the OOI DAS data set. The data collection was  
334 supported by the National Science Foundation under grant OCE-2141047.

335 **References and links**

336 Charif, R. A., Mellinger, D. K., Dunsmore, K. J., Fristrup, K. M., and Clark, C.  
337 W. (2002). “Estimated source levels of fin whale (*Balaenoptera*  
338 *physalus*) vocalizations: Adjustments for surface interference,” Mar.  
339 Mamm. Sci. 18(1), 81-98.

340 Dahl, P. H., Dall'Osto, D. R., and Harrington, M. J. (2021) “Trends in low-  
341 frequency underwater noise off the Oregon coast and impacts of  
342 COVID-19 pandemic,” J. Acoust. Soc. Am. 149, 4073-4077.

343 Dong, B., Popescu, A., Tribaldos, V. R., Byna, S., Ajo-Franklin, J., and Wu, K.  
344 (2022). “Real-time and post-hoc compression for data from Distributed  
345 Acoustic Sensing,” Comput. Geosci. 166, 105181.

346 Duarte, C. M., Chapuis, L., Collin, S. P., Costa, D. P., Devassy, R. P.,  
347 Eguiluz, V. M., ... and Juanes, F. (2021). “The soundscape of the  
348 anthropocene ocean,” Science 371(6529), eaba4658.

349 Hartog, A. H. (2017). “An introduction to distributed optical fibre sensors,”  
350 (CRC press. Boca Raton, Florida), 472 pp.

351 Jensen, F., Kuperman, W., Porter, M., and Schmidt, H. (1994).  
352 “Computational Ocean Acoustics” (American Institute of Physics, New  
353 York), 634 pp.

354 Lewis, L. A., Calambokidis, J., Stimpert, A. K., Fahlbusch, J., Friedlaender,  
355 A. S., McKenna, M. F., ... and Širović, A. (2018). "Context-dependent  
356 variability in blue whale acoustic behaviour," Royal Soc. open Sci.  
357 5(8), 180241.

358 Lindsey, N. J., and Martin, E. R. (2021). "Fiber-optic seismology," Ann. Rev.  
359 Earth Planet. Sci. 49, 309-336.

360 Lindsey, N. J., Dawe, T. C., and Ajo-Franklin, J. B. (2019). "Illuminating  
361 seafloor faults and ocean dynamics with dark fiber distributed acoustic  
362 sensing," Science 366(6469), 1103-1107.

363 McDonald, M. A., Calambokidis, J., Teranishi, A. M., and Hildebrand, J. A.  
364 (2001). "The acoustic calls of blue whales off California with gender  
365 data," J. Acoust. Soc. Am. 109(4), 1728-1735.

366 MacGillivray, A. and de Jong, C. (2021). "A reference spectrum model for  
367 estimating source levels of marine shipping based on automated  
368 identification system data," J. Mar. Sci. Eng. 9(4), 369.

369 Mateeva, A., Lopez, J., Potters, H., Mestayer, J., Cox, B., Kiyashchenko,  
370 D., ... and Detomo, R. (2014). "Distributed acoustic sensing for  
371 reservoir monitoring with vertical seismic profiling," Geophys.  
372 Prospect. 62(4), 679-692.

373 Matsumoto, H., Araki, E., Kimura, T., Fujie, G., Shiraishi, K., Tonegawa,  
374 T., ... and Karrenbach, M. (2021). "Detection of hydroacoustic signals  
375 on a fiber-optic submarine cable," Sci. Rep. 11(1), 1-12.

376 McKenna, M. F., Ross, D., Wiggins, S. M., Hildebrand, J. A. **(2012)**.  
377 “Underwater radiated noise from modern commercial ships,” *J. Acoust.*  
378 *Soc. Am.* 131(1), 92-103.

379 Oleson, E. M., Calambokidis, J., Burgess, W. C., McDonald, M. A., LeDuc,  
380 C. A., and Hildebrand, J. A. **(2007)**. “Behavioral context of call  
381 production by eastern North Pacific blue whales”, *Mar. Ecol. Prog. 330*,  
382 269-284.

383 Rivet, D., de Cacqueray, B., Sladen, A., Roques, A., and Calbris, G. **(2021)**.  
384 “Preliminary assessment of ship detection and trajectory evaluation  
385 using distributed acoustic sensing on an optical fiber telecom cable,” *J.*  
386 *Acoust. Soc. Am.* 149(4), 2615-2627.

387 Sladen, A., Rivet, D., Ampuero, J. P., De Barros, L., Hello, Y., Calbris, G.,  
388 and Lamare, P. (2019). “Distributed sensing of earthquakes and ocean-  
389 solid Earth interactions on seafloor telecom cables,” *Nat. Commun.*  
390 10(1), 1-8.

391 Smith, L. M., Barth, J. A., Kelley, D. S., Plueddemann, A., Rodero, I., Ulses,  
392 G. A., ... and Weller, R. **(2018)**. “The ocean observatories initiative,”  
393 *Oceanogr.* 31(1), 16-35.

394 Stimpert, A. K., DeRuiter, S. L., Falcone, E. A., Joseph, J., Douglas, A. B.,  
395 Moretti, D. J., ... and Goldbogen, J. A. **(2015)**. “Sound production and  
396 associated behavior of tagged fin whales (*Balaenoptera physalus*) in the  
397 Southern California Bight,” *Anim. Biotelemetry* 3(1), 1-12.

398 Taweesintananon, K., Landrø, M., Brenne, J. K., and Haukanes, A. **(2021)**.  
399 “Distributed acoustic sensing for near-surface imaging using submarine

400 telecommunication cable: A case study in the Trondheimsfjord,  
401 Norway," *Geophys.* 86(5), B303-B320.

402 Thode, A. M., D'Spain, G. L., and Kuperman, W. A. (2000). "Matched-field  
403 processing, geoacoustic inversion, and source signature recovery of  
404 blue whale vocalizations," *J. Acoust. Soc. Am.* 107(3), 1286-1300.

405 Watkins, W. A., Tyack, P., Moore, K. E., and Bird, J. E. (1987). "The 20-20 Hz  
406 signals of finback whales (*Balaenoptera physalus*)," *J. Acoust. Soc.  
407 Am.* 82(6), 1901-1912.

408 Weirathmueller, M. J., Wilcock, W. S. D., and Soule, D. C. (2013). "Source  
409 levels of fin whale 20 Hz pulses measured in the Northeast Pacific  
410 Ocean," *J. Acoust. Soc. Am.* 133(2), 741-749.

411 Weirathmueller, M. J., Stafford, K. M., Wilcock, W. S., Hilmo, R. S., Dziak,  
412 R. P., and Tréhu, A. M. (2017). "Spatial and temporal trends in fin  
413 whale vocalizations recorded in the NE Pacific Ocean between 2003-  
414 2013," *PLoS One* 12(10), e0186127.

415 Wilcock, W. S. D., Stafford, K. M., Andrew, R. K., and Odom, R. I. (2014).  
416 "Sounds in the ocean at 1-100 Hz," *Ann. Rev. Mar. Sci.* 6(1), 117-140.

417 Wilcock, W. S. D., and Hilmo, R. S. (2021). "A method for tracking blue  
418 whales (*Balaenoptera musculus*) with a widely spaced network of ocean  
419 bottom seismometers," *PLoS One* 16(12), e0260273.

420 Williams, E. F., Fernández-Ruiz, M. R., Magalhaes, R., Vanthillo, R., Zhan,  
421 Z., González-Herráez, M., and Martins, H. F. (2019). "Distributed  
422 sensing of microseisms and teleseisms with submarine dark fibers,"  
423 *Nat. Commun.* 10(1), 1-11.

424 Zhan, Z. (2019). "Distributed Acoustic Sensing Turns Fiber- Optic Cables  
425 into Sensitive Seismic Antennas," *Seismol. Res. Lett.* 91, 1–15.